Chapter 4
A Kinetic Model for Predicting Polymeric Neutron Shieldings Lifetime

F. Nizeyimana and H. Issard

Abstract Polymers are widely used in radioactive material transport/storage casks. Their neutron shielding ability relies mostly on their concentrations in hydrogen atoms which slow down neutrons. However, in-service high temperatures are responsible for H abstraction decreasing polymers shielding capability. Therefore, their long-term properties must be accurately predicted. In this regard, a multi-year R&D program has been set up to elucidate oxidation mechanisms of neutron shielding materials and develop a nonempirical lifetime prediction methodology. This paper deals with accelerated aging tests and modeling of a vinylester based neutron shielding product, commercially known as *TN Vyal B*™. Samples are exposed to various temperatures up to 160 °C and O_2 partial pressure and analyzed using various experimental techniques. Basically, thin free films are fully oxidized while thick samples show the diffusion-limited oxidation (DLO): a superficial layer is oxidized whereas the core is not affected. Therefore, to investigate the long-term properties, it is obvious that DLO phenomenon must be taken into account by coupling both oxidation kinetic and oxygen diffusion. In our case, there is a good agreement between simulated weight losses and oxidation thicknesses. Based on degradation assessment and design temperature of dry storage casks, *TN Vyal B*™ excellent resistance can be confirmed.

Keywords Neutron shielding • Polymer • Vinylester composite • Dynamic mechanical analysis • Glass transition • FTIR • µATR • Oxidized layer profiling • Aging • Diffusion limited oxidation • High temperature • Gravimetric analysis • Kinetic mechanism • Modelling • Simulated data • Long-term performance

---

F. Nizeyimana (✉) • H. Issard
AREVA TN International, 1, rue des hérons, Montigny Le Bretonneux,
78 054 Saint Quentin en Yvelines, France
e-mail: fidele.nizeyimana@areva.com

C.C. White et al. (eds.), *Service Life Prediction of Exterior Plastics: Vision for the Future*, DOI 10.1007/978-3-319-06034-7_4

Introduction

Polymeric resins are widely used thanks to their versatility. In aeronautic applications, they are chosen to replace metallic components for mass and cost reduction. In automobile industry, they are nowadays present in numerous cars components as well as paints. Other important applications for polymers are offshore industry (boats shells), civil engineering (concretes, electrical cables insulators…), to name a few.

In our case, the polymer resin based composite is used as a neutron shielding in radioactive material transport/storage casks. Over service life of the casks, initial properties of neutron shielding may fall due to thermal oxidation and neutron radiation. To our knowledge, degradation of shielding polymers via neutron radiation is insignificant. However, oxidation effects can be dramatic and irreversible, especially for the very long-term service. Thermal oxidation reactions are associated with crosslinking, chain scission, hydrogen atoms abstraction, leading to oxidation products buildup. These products are generally concentrated in a thin superficial layer.

Long-term properties are commonly assessed using an Arrhenius model. However, controversies related to the use of these models have been reported [1, 2]. Gillen et al. [1] examined risks taken by considering the same activation energy (Ea) for a great range of temperatures (even a narrow change in Ea affects extrapolated predictions). Their work also shows another important mechanism that leads to a non-Arrhenius behavior, involving diffusion-limited oxidation (DLO).

Recently, to simulate oxidation aging more confidently, new methodologies have been derived [3–6]. In this paper, the time–temperature behavior will be clarified using results obtained by optical microscopy and Micro-ATR analysis. Furthermore, from Arrhenius limitations stated above, TN International has adopted a new and accurate model for predicting its neutron shielding polymeric materials. The model is derived from a mechanistic scheme [7] coupled with Fick 2nd law, $\frac{\partial[O_2]}{\partial t} = D\frac{\partial^2[O_2]}{\partial z^2}$. The same approach has been previously developed and applied to epoxies [3, 5, 6], bismaleimides [4], to name a few. The aim of this paper is to demonstrate the robustness of this nonempirical model on a vinylester resin based neutron shield, *TN Vyal B*™.

Theoretical Calculations and Modeling

Our kinetic model methodology is based on a kinetic mechanism and O_2 diffusion permeation parameters.

(a) *Schematic mechanism*

This mechanism is derived from scheme proposed by British scientists Bolland and Gee [7]. It is possible to divide the scheme in three steps: initiation, propagation, and termination. Without getting into further details, the derivative scheme is described below. To our knowledge, unfortunately, no other nuclear actor has implemented this methodology, even though, the neutron shielding materials are required to last decades in service.

During the first step, ***initiation***, hydroperoxides (POOH) are decomposed free radicals (PO°, OH°, PO°, P°):

$$\mathrm{POOH} \rightarrow \mathrm{PO}^{\circ} + \mathrm{OH}^{\circ} \qquad \text{(ii)}$$

$$\mathrm{PO}^{\circ} + \mathrm{PH} \rightarrow \mathrm{POH} + \mathrm{P}^{\circ} \qquad \text{(iii)}$$

$$\mathrm{OH}^{\circ} + \mathrm{PH} \rightarrow \mathrm{H_2O} + \mathrm{P}^{\circ} \qquad \text{(iv)}$$

Radicals can reorganize with β-scission in either carbonylated (P = O) or alcoholic (POH) products:

$$\begin{array}{l} \mathrm{x\,PO}^{\circ} + \mathrm{x\,PH} \rightarrow \mathrm{x\,POH} + \mathrm{P}^{\circ} \quad (\mathrm{j}) \\ (1-\mathrm{x})\mathrm{P0}^{\circ} \rightarrow (1-\mathrm{x})\mathrm{P} = 0 + (1-\mathrm{x})\mathrm{P}^{\circ} \quad (\mathrm{jj}) \\ \hline \mathrm{POOH} + (1+\mathrm{x})\mathrm{PH} \rightarrow 2\,\mathrm{P}^{\circ} + \mathrm{H_2O} + \mathrm{x\,POH} + (1-\mathrm{x})\mathrm{P} = \mathrm{O} \qquad k_1 \quad (1) \end{array}$$

It is worth noting that a few of the products P = O and POH are volatile and together with water, they are responsible for oxidation-induced mass loss. They are denoted by “V” in initiation reaction:

$$\mathrm{POOH} + 2\,\mathrm{PH} \rightarrow 2\,\mathrm{P}^{\circ} + \mathrm{H_2O} + {}^{-}\mathrm{V} \qquad k_1 \qquad \text{Initiation} \quad (1)$$

The ***propagation*** step follows with two reactions taking place; the first reaction consists in combination of O_2 and P° radicals yielding a new radical PO_2°. While the latter react with polymer to produce hydroperoxides and P° radicals. Propagation reactions are given below:

$$\mathrm{P} + \mathrm{O_2} \rightarrow \mathrm{PO_2} \qquad k_2 \qquad \text{Propagation} \quad (2)$$

$$\mathrm{PO_2} + \mathrm{PH} \rightarrow \mathrm{POOH} + \mathrm{P} \qquad k_3 \qquad \text{Propagation} \quad (3)$$

Besides, free radicals could react with each other, yielding stable (inactive) species. This process is known as ***termination***:

$$\mathrm{P} + \mathrm{P} \rightarrow \text{inactive products} \qquad k_4 \qquad \text{Termination} \quad (4)$$

$$\mathrm{P} + \mathrm{PO_2} \rightarrow \text{inactive products} \qquad k_5 \qquad \text{Termination} \quad (5)$$

$$\mathrm{PO_2} + \mathrm{PO_2} \rightarrow \text{inactive products} + \mathrm{O_2} \quad k_6 \qquad \text{Termination} \quad (6)$$

From the chemical scheme detailed above, a system of differential equations can be set to describe all species concentrations over aging time.

$$\frac{\mathrm{d}[\mathrm{P}^\circ]}{\mathrm{d}t} = 2k_1[\mathrm{POOH}] - k_2[\mathrm{O}_2][\mathrm{P}^\circ] + k_3[\mathrm{PH}][\mathrm{PO}_2{}^\circ] - 2k_4[\mathrm{P}^\circ]^2 - k_5[\mathrm{P}^\circ][\mathrm{PO}_2{}^\circ] \quad \text{(I)}$$

$$\frac{\mathrm{d}[\mathrm{PO}_2{}^\circ]}{\mathrm{d}t} = k_2[\mathrm{O}_2][\mathrm{P}^\circ] - k_3[\mathrm{PH}][\mathrm{PO}_2{}^\circ] - k_5[\mathrm{P}^\circ][\mathrm{PO}_2{}^\circ] - 2k_6[\mathrm{PO}_2{}^\circ] \quad \text{(II)}$$

$$\frac{\mathrm{d}[\mathrm{POOH}]}{\mathrm{d}t} = -k_1[\mathrm{POOH}] + k_3[\mathrm{PH}][\mathrm{PO}_2{}^\circ] \quad \text{(III)}$$

$$\frac{\mathrm{d}[\mathrm{PH}]}{\mathrm{d}t} = -k_3[\mathrm{PH}][\mathrm{PO}_2{}^\circ] - 2k_1[\mathrm{POOH}] \quad \text{(IV)}$$

$$\frac{\mathrm{d}[\mathrm{O}_2]}{\mathrm{d}t} = -k_2\mathrm{O2}[\mathrm{P}^\circ] + k_6[\mathrm{PO}_2{}^\circ]^2 + D\frac{\partial^2[\mathrm{O}_2]}{\partial z^2} \quad \text{(V)}$$

It should be emphasized that the final equation (Eq. V) is composed of two terms. The first, $-k_2\mathrm{O}_2[\mathrm{P}^\circ] + k_6[\mathrm{PO}_2{}^\circ]^2$, corresponds to O_2 consumption and the second to Fick's 2nd law, $\frac{\partial[\mathrm{O}_2]}{\partial t} = D\frac{\partial^2[\mathrm{O}_2]}{\partial z^2}$, where D is O_2 diffusion and $[O_2]$ represents O_2 concentration in depth x.

$[O_2]$ values shift from equilibrium concentration (C_s) on samples surface to nil in the core. C_s is given by Henry's law: $C_s = S_{O_2} \times p_{O_2}$, where S is O_2 solubility in the polymer and p the O_2 partial pressure. Parameters D and S are obtained experimentally by permeation tests. They are given in Table 4.1.

The set of differential equations written above were solved numerical by the finite difference method of Runge–Kutta (Ode23tb of Matlab). Basically, a polymer sample is discretized into N knots equally spaced with a distance Δx:

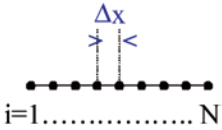

(Lines $i = 1$ and $i = \mathrm{N}$ correspond to both surfaces of the sample).

$$\textit{Initial conditions}(t=0), i = 1,\ldots,\mathrm{N}; [\mathrm{P}^\circ]=0; [\mathrm{PO}_2{}^\circ]=0; [\mathrm{PH}]=[\mathrm{PH}]_{0;}$$
$$[\mathrm{POOH}]=[\mathrm{POOH}]_0$$

Table 4.1 Oxygen parameters used in our model

T (°C)	120	140	160
D 10^{-12} (m^2s)	3.9	4.9	6.0
C_s (atmospheric pressure)	3.5×10^{-4} mol/l		
C_s (2×10^5 Pa)	3.5×10^{-3} mol/l		

For each time $t > 0$; $i = 1, \ldots, N$, the system of differential equations can be rewritten as follow:

$$\frac{d[P^\circ]}{dt}i = 2k_1[POOH]_i - k_2\,C_i[P^\circ]_i + k_3[PH]_i[PO_2{}^\circ]_i - 2k_4[P^\circ]_i^2 - k_5[P^\circ]_i[PO_2{}^\circ]_i$$

$$\frac{d[PO_2{}^\circ]}{dt}i = k_2C_i[P^\circ]_i - k_3[PH]_i[PO_2{}^\circ]_i - k_5[P^\circ]_i[PO_2{}^\circ]_i - 2k_6[PO_2{}^\circ]_1^2$$

$$\frac{d[POOH]}{dt}i = -k_1[POOH]_i + k_3[PH]_i[PO_2{}^\circ]_i$$

$$\frac{d[PH]}{dt}i = -k_3[PH]_i[PO_2{}^\circ]_i - 2k_1[POOH]_i$$

The weight variation is calculated taking into account the reaction I (initiation) that leads to water yield, volatile products, as well as O_2 grafting on polymer chains during oxidation process:

$$\frac{1}{m_0}\frac{dm}{dt} = \underbrace{\frac{32}{\rho_0}R(C)}_{\text{mass uptake due } O_2 \text{ uptake}} - \underbrace{\frac{18}{\rho_0}\frac{d[H_2O]}{dt} - \frac{M_V}{\rho_0}\frac{d[V]}{dt}}_{\text{mass loss : water and oxidation products}}$$

$$R(C) = k_2C[P^\circ] - k_6[PO_2{}^\circ]^2$$

Experimental

Material

The material is a TN International patented polymer composite, *TN Vyal B*™, here after referred to as a vinylester composite.

Its polymer matrix, vinylester resin, can be affected by long-term exposure in severe conditions. Prior to aging tests, matrix films (30 µm < thickness < 45 µm) and composite thick samples (0.5 mm < thickness <2 mm) were cured at 80 °C for 12 h and post-cured at 160 °C for 2–4 h. Following this process, the material's cure is enhanced and unreacted free species are eliminated.

Measurements

Samples were exposed between 120 and 160 °C in pure oxygen at partial pressure of 2×10^5 Pa and atmospheric pressure. Then, various chemical, physical, and mechanical characterizations were performed on the industrial neutron shielding (vinylester composite). To confirm or go further into understanding of observed phenomena, specific and limited analyses were done on the vinylester matrix free films.

(a) Gravimetric analysis
Gravimetric analysis was carried out periodically over aging time using a balance with a relative accuracy of 10^{-4}. Weight changes were calculated as follows:

$$\frac{m}{m_0}(\%) = \frac{m_t - m_0}{m_0} \times 100 \quad \text{with } m_0, m_t \text{ corresponding to initial weight and weight at aging time } t, \text{ respectively.}$$

(b) Infrared Spectroscopy
Two methods of IR measurements were carried out. First of all, IR spectra were collected in the region 4,000–400 cm^{-1} directly on matrix free films (30–40 μm of thickness). The FTIR machine used was a Brucker IFS 28 Spectrometer. Spectra were recorded in a transmission mode with an average of 32 scans. To determine species concentration, C (expressed in mol/l), Beer–Lambert law was applied:

$$C = \frac{A}{\varepsilon l'} \quad \text{where } A \text{ is absorbance and } \varepsilon \text{ and molar absorptivity and sample s thickness respectively.}$$

The second method was Micro-ATR Spectroscopy where a Spotlight 300 apparatus coupled with Spectrum 100 FTIR Spectrometer is used. With this technique, IR spectra are recorded in the entire oxidized layer. Two of the peaks which presented noticeable changes were particularly monitored:

- 1,727 cm^{-1} which seemed to increase in absorbance during aging
- 1,145 cm^{-1} which only appeared after samples exposure

Then, the obtained profiles were compared to the prediction.

(c) Dynamic mechanical analysis (DMA)
This method provides a comprehensive understanding of material's internal molecular mobility, over aging time as well as structural changes. Plus, glass temperature (*Tg*) changes over aging time gives an interesting information on residual crosslinking or even post-cure taking place due to aging processes.

Measurements were conducted on 2 mm thick samples using a NETZCH DMA 242 instrument in a tensile mode. Measurements conditions are listed below:

Temperature scans between 30 and 200 °C
Heating rate of 5 °C/min
Frequency of 1 Hz

As there's no standard of determining *Tg*, its values can be monitored as an offset of storage modulus, E', or on maxima of loss modulus E'' and loss tangent, tanδ. In our case, *Tg* data were collected on E′.

Results and Discussion

Identification of Structural Changes

Measurements on free films were carried out to assess changes in the vinylester matrix network over time. Figure 4.1 displays the comparison between IR spectra of a film at t_0 and after its exposure to 160 °C under 2×10^5 Pa for 645 h.

The main spectra modifications are given below:

- Slight decrease of C–H at 2,935 cm^{-1} due to H abstraction during oxidation process
- Significant increase in intensity of 1,725 cm^{-1} peak due to "new" carbonyl groups (C = O) build up
- Broadening of 1,244 cm^{-1} peak (aromatic C–O) suggesting complex molecular rearrangements
- The peak corresponding to C–O methacrylate at 1,180 cm^{-1} shifts to lower wavelength number (1,170 cm^{-1})

As shown in Fig. 4.2a, carbonyl groups (C = O) buildup increases steadily until over 650 h, then stabilizes with aging time. In addition, evolution of the new peak that appeared at 1,170 cm^{-1} after exposure is presented in Fig. 4.2b. It was quantified by rationing its absorbance with the internal reference at 1,494 cm^{-1} (related to stable aromatic C = C bonds). Its evolution displays a sharp increase after only 50 h followed by a slight and progressive increase up to around 400 h. All of this IR results suggest that oxidation is time-dependent process. They also reveal that C–H oxidation depends on its position in the polymer chain. Hence, C–H in α-position to

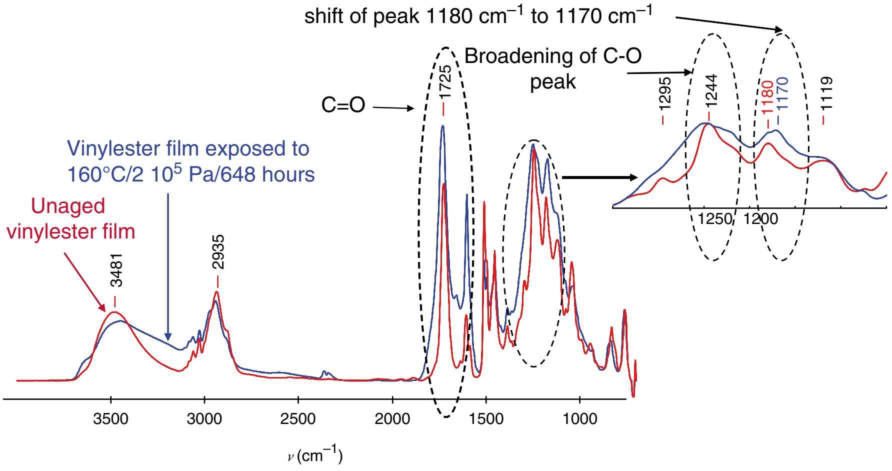

Fig. 4.1 FTIR spectra of a vinylester free film: (**a**) before aging; (**b**) after exposure to 160 °C under 2×10^5 Pa of O_2 for 648 h

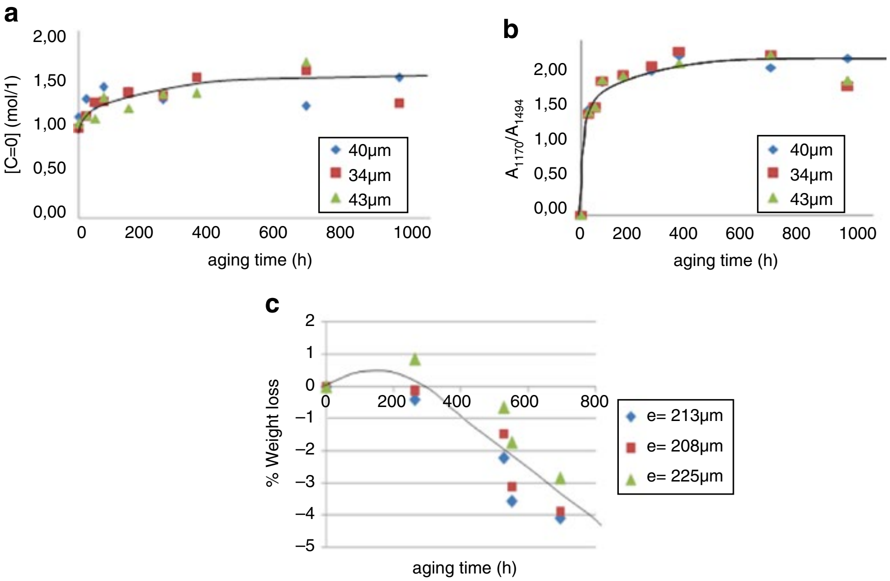

Fig. 4.2 Evidence of free films degradation: (**a**) carbonyl groups (C = O) buildup; (**b**) increase of the peak at 1,170 cm^{-1}; (**c**) variation of films weight

oxygen (–$\mathbf{CH_2}$–O–) or tertiary (–CH_2–$\mathbf{CH}$–CH_3) are oxidized quite rapidly, and, consequently, concentration oxidation products also increase rapidly. That is what is observed during the first hours of aging. Finally, relative stability observed after 650 h does not mean that oxidation has stopped. In fact, one could be aware that, at this stage, there is a competition between oxidation and evaporation of a part of volatile oxidation products.

By gravimetric analysis showed in Fig. 4.2c, two steps are observed. The slight mass uptake observed until 200 h indicate the grafting of oxygen atoms on polymer chains during the second reaction of propagation. It is worth mentioning that this step wasn't observed for composite samples, probably due to early predominance of evaporation (weight loss) over mass uptake. The sharp weight loss at higher duration indicates once again the evaporation of volatile oxidation products stated above.

In addition of FTIR and gravimetric analysis, structural changes were also evaluated with DMA analysis performed on vinylester composite exposed to different temperatures and O_2 partial pressure. The results are shown in Fig. 4.3.

Quite interestingly, the evolution of *Tg* seems to follow a "master curve" whatever the aging conditions. *Tg* quick increase is seen before 100 h where it reaches roughly 150 °C. Then, *Tg* increases progressively to an "indefinite" value or *Tg*∞ of 170 °C. This result is a good indication of a post-cure related to recombination of radicals generated by oxidation. Meanwhile, over 1,200 h, *Tg* seems to decrease slightly. Even if this decrease is less significant, an important question can be raised here: are there any chain scission reactions that may lead to a drop of crosslinking density at higher exposure durations?

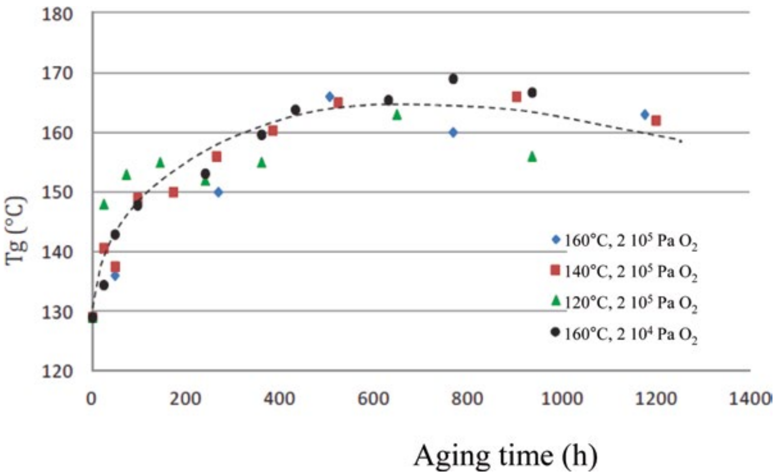

Fig. 4.3 The change in *Tg* of vinylester composite during its exposure to different temperatures and O_2 pressure

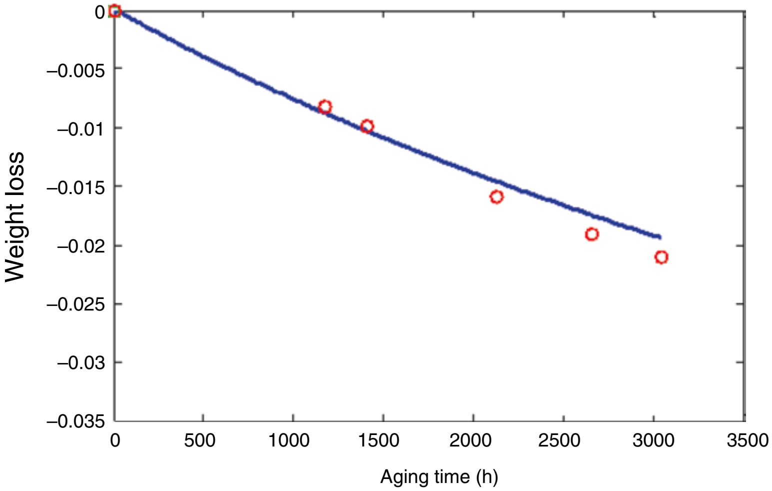

Fig. 4.4 Weight loss curve obtained for vinylester composite at 140 °C under 2×10^5 Pa of O_2: experimental (**o**), model (—)

Weight Loss Modeling

The kinetic model was used to predict oxidation-induced weight loss for samples exposed to different temperatures and oxygen pressure. For instance, in Fig. 4.4, a quite acceptable agreement is shown for composite samples exposed to 140 °C and 2×10^5 Pa of O_2.

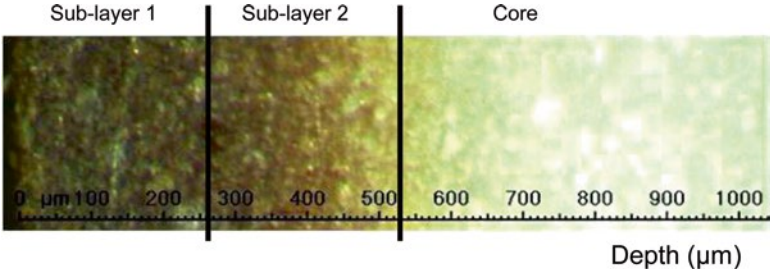

Fig. 4.5 Optical photography of a composite sample (thickness = 2 mm) exposed to 160 °C/2×10^5 Pa of O_2 for 1,200 h

Oxidation Layers Profiling

As mentioned earlier, only superficial layer is affected by samples exposure to oxidative environment. This phenomenon is qualitatively shown in Fig. 4.5 for samples aged at 160 °C/2×10^5 Pa of O_2. Degradation is symmetrical relative to the center; therefore, only half the sample is shown.

By optical microscopy, color heterogeneities or gradient in sample thickness are easily observed confirming the existence of diffusion-controlled oxidation. First of all, from the sample's edge, a layer of roughly 250 µm is browned (sub-layer 1) followed by a yellowing of around 250 µm (sub-layer 2) while the core of the sample has kept its original color. Therefore, based on this experimental technique, overall oxidation layer can be estimated to extend to a depth of 500 µm.

On the other hand, using µATR, oxidation layers were also successfully determined by measuring the concentration of oxidation products for all studied aging conditions. They were compared to profile prediction.

Figure 4.6 displays a three-dimensional (3D) presentation of degradation using our model. As expected, oxidation products buildup showed an exponential evolution with the higher concentration on sample's edge decreasing continually to the core.

Overall, the higher the aging temperature, the greater was the oxidation layer thickness. For instance, in Fig. 4.7, oxidized layer profiles of samples aged separately for around 1,200 h at 160 °C 2×10^5 Pa of O_2 and atmospheric pressure are presented. As can be seen, for the same aging temperature, oxidized thickness is roughly doubled when the pressure is increased from atmospheric pressure to 2×10^5 Pa. Finally and most interestingly, it is clear that there's a relative good agreement between simulated and experimental profiles obtained by µATR.

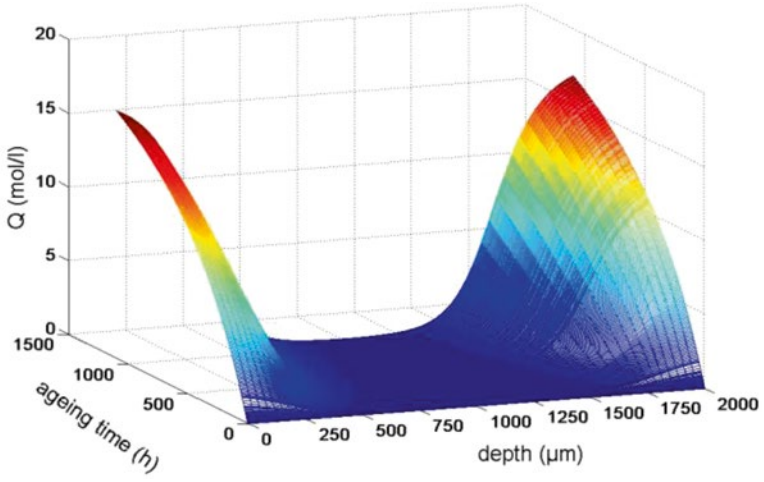

Fig. 4.6 3D presentation of predicted OL profile of TN Vyal B™ exposed at 160 °C/2 × 10^5 Pa O_2 for 1,200 h

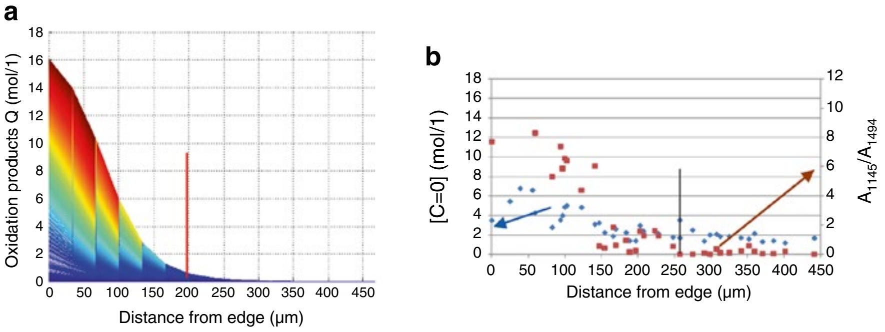

160°C/2 10^5 Pa O_2: (a) model, (b) experimental

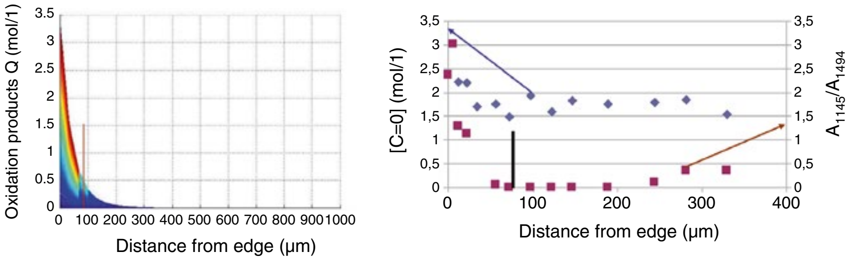

160°C under atmospheric pressure: (a) model, (b) experimental

Fig. 4.7 Example of simulated and experimental oxidized layer thickness for composite samples exposed to 160 °C/2 × 10^5 Pa O_2 and atmospheric pressure for 1,200 h. 160 °C/2 × 10^5 Pa O_2: (**a**) model, (**b**) experimental. 160 °C under atmospheric pressure: (**a**) model, (**b**) experimental

Conclusion

The material studied is a TN International vinylester based neutron shielding product, commercially known as *TN Vyal B*™. The focus of our study was to investigate the material's thermal degradation mechanism using accelerated aging tests and to validate a nonempirical model for predicting long-term in-service properties. Conclusions are the following:

- Aging leads to superficial oxidative layer buildup suggesting a DLO effect. IR measurements show a slight decrease of C–H groups (hydrogen abstraction) followed by an increase in carbonyl groups in the oxidized layer
- Exposure of free films to high temperatures and oxygen caused early mass uptake (due to O_2 grafting on polymer chain) followed by a dramatic drop of mass (due to volatile oxidation products). For composite, however, mass uptake is very rapid and difficult to be monitored
- In the initial exposure time, *Tg* increases due to post-cure. At longer exposures, *Tg* starts to decrease due to some polymer chain scission
- A good correlation of experimental and simulated data is obtained on weight changes as well as oxidation profiles
- The new approach allows a great understanding of our neutron shielding long-term performance

Acknowledgment This work was supervised in part by V. Bellenger who is greatly acknowledged.

References

1. Gillen KT, Celina M, Clough R, Wise J (1997) Extrapolation of accelerated aging data – Arrhenius or Erroneous? Trends Polym Sci 5(8):250–257
2. Celina M, Gillen KT, Assink RA (2005) Accelerated aging and lifetime prediction: review of non Arrhenius behavior due to two competing processes. Polym Degrad Stab 90:395–404
3. Colin X, Marais C, Verdu J (2001) A new method for predicting the thermal oxidation of thermoset matrices: application to an amine crosslinked epoxy. Polym Test 20:795–803
4. Colin X, Marais C, Verdu J (2002) Kinetic modelling and simulation of gravimetric curves: application to the oxidation of bismaleimide and epoxy resins. Polym Degrad Stab 78:545–553
5. Bellenger V, Decelle J, Huet N (2005) Ageing of a carbon epoxy composite for aeronautic application. Compos Part B 36(3):189–194
6. Bellenger V, Verdu J (1985) Oxidative skeleton breaking in epoxy-amine networks. J Appl Polym Sci 30:363–374
7. Bolland JL, Gee G (1946) Kinetic studies in the chemistry of rubber and related materials. Trans Faraday Soc 42:236–243